

# Passive RF in Support of LEO Orbit Determination

**Kameron Simon**

*Kratos*

**Steve Williams**

*Kratos*

**Ian Hersom**

*Kratos*

## ABSTRACT

In today's already contested and congested space environment, the proliferation of Low Earth Orbit (LEO) satellites only increases the need to identify, characterize, and track satellites to maintain Space Domain Awareness (SDA). This paper will explore applying passive Radio Frequency (RF) techniques that could be used to uniquely identify, characterize, and track objects in LEO. Traditional techniques utilize electro-optical and radar sensors, but each of these have their own advantages and limitations. Electro-optical techniques may perform well during the night but become less efficient during daylight, inoperable during cloudy conditions, and are hampered by lightning strikes. Electro-optical sensors also have a difficult time distinguishing between objects of similar size (i.e., cubesat visual magnitudes) or closely spaced objects. Satellite operators are starting to experiment with sunshades or black coatings avoiding problems with providing too bright of background for astronomers as seen with Space X. This makes it next to impossible for electro-optical techniques to identify or track these objects. While radar is generally effective in all-weather conditions, day or night, it has difficulty distinguishing between objects of similar size and shape (i.e., cubesat radar cross-sections). Passive RF can perform in all-weather conditions, day or night and can uniquely identify actively transmitting objects even if they are the same in size, shape, and brightness, or are closely spaced, by using the transmitted signal.

This paper will explore how passive RF can be used to blind-scan satellites to identify and characterize the signals being transmitted from the satellite, since all active satellites transmit a signal to either provide TT&C, data, or communications. The methods explored in this paper are useful in uniquely identifying satellites that are launched in large clusters. The paper will additionally explore a method to track the signals identified for a particular satellite and use that information to create or refine an orbital state vector. At the conclusion, the reader will recognize how passive RF helps SDA to identify, characterize and track satellites in LEO constellations from launch through the satellite's end of life.

## 1. INTRODUCTION

As the proliferation of Low Earth Orbit (LEO) satellite constellations continues to grow so does the need to correctly locate, identify, characterize, differentiate, and track those satellites. The ability to identify and track these objects helps maintain Space Domain Awareness (SDA) to aid in safety of flight for all satellites. While there are existing phenomenologies to do this today, each has its strengths and weaknesses.

- Electro-optical techniques may perform well during the night but become less efficient during daylight, inoperable during cloudy conditions, and are hampered by lightning strikes. Electro-optical sensors also have a difficult time distinguishing between objects of similar size (i.e., cubesat visual magnitudes), or closely spaced objects. Satellite operators are starting to experiment with sunshades or painting satellites black as to not impact astronomers as seen with Space X. This makes it next to impossible for electro-optical techniques to identify or track these objects.
- Radar techniques are generally effective in all-weather conditions, day or night, and have great accuracy. Radar has difficulty distinguishing between objects of similar size and shape (i.e., cubesat radar cross-sections). Radar sensors also have difficulty with long distances or small objects.

- Passive RF techniques, while able to correctly locate, identify, characterize, and track satellites are not without their limits, as they require satellites to be transmitting active signals to track. This means passive RF cannot be used to track space debris.

Table 1 shows a comprehensive list of how the three phenomenologies (electro-optical, radar, passive RF) compare in different tracking capabilities.

Table 1 Space Tracking Phenomenology Capability Overview

<i>Capability</i>	<b>Optical</b>	<b>Radar</b>	<b>Passive RF</b>
<i>Nighttime Tracking</i>	●	●	●
<i>Daylight Tracking</i>	●	●	●
<i>All-weather Tracking</i>	●	●	●
<i>Debris Tracking</i>	●	●	●
<i>LEO Satellites</i>	●	●	●
<i>MEO Satellites</i>	●	●	●
<i>GEO Satellites</i>	●	●	●
<i>Cislunar Satellites</i>	●	●	●
<i>Launch / Early Orbit Tracking</i>	●	●	●
<i>Low-Reflectivity RSOs</i>	●	●	●
<i>Differentiate RSOs of Similar Shape and Size</i>	●	●	●
<i>Rendezvous / Proximity Operations</i>	●	●	●
<i>Specific Emitter Identification (SEI)</i>	●	●	●
<i>Measure RF Comms and Interference</i>	●	●	●
<i>Geolocate Terrestrial Signal Sources</i>	●	●	●

Based on Table 1, no single phenomenology accurately depicts what is going on in space; therefore, all phenomenologies are required for true SDA and safety of flight. The following sections will overview how passive RF can support SDA of proliferated LEO satellites by providing different ways to identify, characterize and track satellites.

## 2. PASSIVE RF OVERVIEW

Passive RF utilizes the RF signals transmitted by the satellite, characterizing each satellite as the RF signal emitted is like a human fingerprint and is unique to each satellite. The RF signals can also be used to determine the position and velocity (i.e., ephemeris). These RF signals can be satellite communications (SATCOM) signals that are re-transmitted by a transponder on the satellite, they can be telemetry signals that are transmitted directly by the satellite, or they can be data downlink signals.

Traditional passive RF ranging requires the RF signal to be received by at least three ground antennas located at least several hundred miles apart from each other for Geosynchronous orbits (GEO). Future sections will show how passive RF can be used to:

- Identify/Characterize – Specific Emitter Identification (SEI) exploits the unintentional characteristics and perturbations of individual RF transmitters to uniquely identify the transmitters by analyzing their transmitted signals. This is very similar with how humans are identified by their fingerprints. These transmitted signal “personalities” occur because of design and manufacturing differences between satellites, specifically in their digital-to-analog converters, frequency mixers, power amplifiers and other RF equipment. SEI generally requires only one ground site, although results can be improved with multiple

sites. SEI implementation with RF Machine Learning (RFML) techniques is an area of active research, experimentation, and field trials with very encouraging results.

- Tracking – There are two primary methods to track a satellite using passive RF. The first uses Time Difference of Arrival (TDOA) and Frequency Difference of Arrival (FDOA). The second uses the Doppler Shift resulting from the satellite’s motion or acceleration caused by maneuvers.
  - TDOA/FDOA - Typically, there are three antenna sites are positioned so that they are separated both latitudinally and longitudinally. This ensures that difference of arrival (DOA) measurements can be taken in both the in-track and cross-track directions of the satellite, which reduces orbit determination (OD) errors in both directions. TDOA values indicate how much longer the RF signal took to arrive at one site relative to another site. This corresponds to the difference in distance from the satellite to each site. FDOA values indicate the difference in received Doppler shift between one site relative to another site and corresponds to the difference in relative speed between the satellite and each site.
  - Doppler Shift – This is experienced when a satellite emitting a RF signal has velocity relative to a ground site. The signal’s wavelength will be shortened or lengthened, depending upon whether the satellite is moving towards or away from the ground site. This change is Doppler Shift and can be measured with a single site measuring a single signal. The Doppler Shift can then be used to create a range-rate. The range rate can then be used in a non-linear OD program. This is a new theoretical technique evaluated in this paper.

Both passive RF tracking methods create measurements that are taken repeatedly over time and are then fed into a non-linear OD process. The OD process produces a state vector (SV) which describes the satellite’s position and velocity at a specific time. Paired with a propagation model, this SV can be used to predict future positions of the satellite. This allows for the information to be used for SDA and safety of flight in conjunction messages.

Utilizing the passive RF tracking/characterization methods and tracking methods it is possible to achieve SDA for safety of flight.

### 3. PASSIVE RF IDENTIFICATION AND CHARACTERIZATION

There are multiple ways to achieve identification and characterization using passive RF data. To date most of this has been done by people analyzing collected spectrum and noticing abnormalities in the signals or noise floor caused by imperfect hardware in the RF path. The abnormality in the data was then used to uniquely identify the spacecraft. However, as spacecraft evolve and move to more digital infrastructure it gets harder to distinguish the abnormalities caused by hardware. This is where the advances in machine learning (ML) have become quite useful, specifically Neural Networks (NN). Fig. 1 is an example of a spectrum plot of satellite KPLO (53365) provided by Clearbox Systems. The reader can easily see the unique frequency at the center of the plot. Each satellite will require a separate frequency or share a frequency between a group. This enables passive RF systems to uniquely identify satellites by the tracking, telemetry, and command (TT&C) signals.

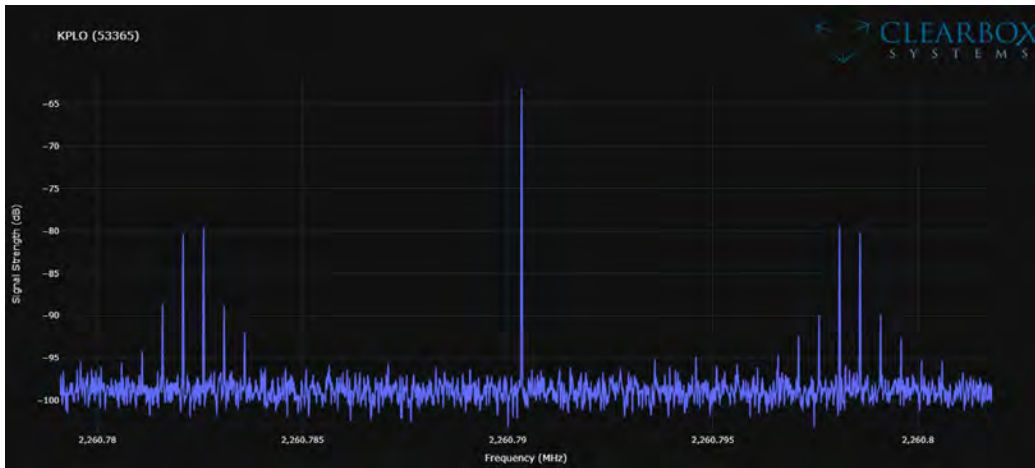


Fig. 1. Spectrum Plot Satellite KPL0

Neural Network (NN) detection and identification of RF fingerprints as an SEI technique, is the subject of significant active research, development, and testing published in the open literature. As an example, Fig. 2 depicts proof-of-concept results from a RFML effort conducted by the Hume Center for National Security and Technology at Virginia Tech University. It shows the gain offset separation (or, in other words “feature amplitude offset”) needed between transmitters to achieve 80, 90, and 95% probabilities of correct identification of a specific transmitter.

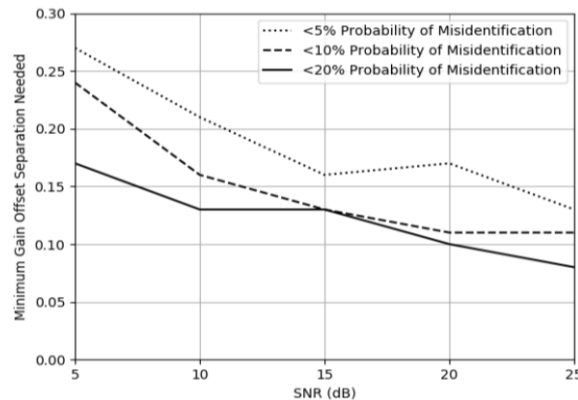


Fig. 2. Probability of Correct Identification of Transmitters [1]

Fig. 2 shows, in general, that the probability of correct identification improves as the fingerprint differences between transmitters increase (moving up the y-axis) and/or as the Signal-to-Noise ratio (SNR) increases (moving to the right on the x-axis). Although this is only one example, it is representative of today’s SEI approaches, and it reveals the power of NNs to identify specific transmitters utilizing RF fingerprints. NN-based SEI is agnostic to signal modulation and does not require excessive over-sampling and dynamic range which are often required by the traditional expert-defined, e.g., human Subject Matter Expert (SME) feature detection. Further, the results shown in Fig. 2 were obtained by feeding the NN a mere 1024 samples of raw I/Q samples.

Typically, NN performance is highly dependent upon exhaustive training with a representative emissions data set from the transmitters to be identified. This is potentially problematic when identifying non-cooperative transmitters since there may be little data available. However, NN-based SEI capabilities can accommodate the identification of as-yet unseen/unknown transmitters for which the system has not been trained. To address this challenge, the process involves deciding when incoming fingerprints are sufficiently different from the existing set of reference/training data such that they indicate the presence of a new transmitter. Then, the approach trains to identify a statistically significant divergence in RF signature features from the existing reference sets.

NN-based RFML performance for SEI is often shown with confusion matrices, as in Fig. 3.

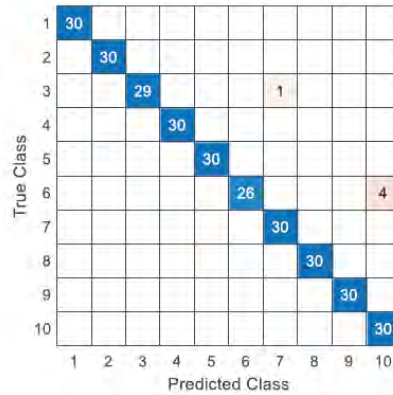


Fig. 3. Confusion Matrix of NN-based SEI Performance [2]

Confusion matrices help to visualize the performance of a machine learning classifier when the true transmitter classes are known. Perfect performance is achieved when the NN blindly classifies each transmitter correctly and is visualized by a single diagonal line across the matrix, e.g., the blue squares, with test count values in each cell. In this example, the NN-based performance outperformed the traditional SEI technique of expert feature analysis.

#### 4. PASSIVE RF TRACKING

There are two main approaches for tracking using passive RF. The first method is the traditional method of TDOA/FDOA tracking. The second method is Doppler Shift tracking.

##### *TDOA/FDOA Tracking*

This section will assess how traditional TDOA/FDOA could be used to track satellites in LEO orbits. This has not yet been done in practice and is therefore simulation-based in this paper to determine if using the method in LEO is feasible and what type of site configuration is necessary to track a LEO satellite's orbit. The data simulated here used an old orbit location for a Starlink satellite.

- Satellite:
  - Starlink-1257 (NORAD ID: 45402)
    - Epoch: 2020-09-12 18:00:15 UTC
    - X: -5500805.8784073368 (m)
    - Y: 3590624.2939960845 (m)
    - Z: 2193851.0305698211 (m)
    - Xdot: -1060.9082903965 (m/s)
    - Ydot: -5045.4521102592 (m/s)
    - Zdot: 5570.2825003079 (m/s)
- Orbit Perturbations:
  - (50x50) EGM-96 Earth Gravity Model
  - 3<sup>rd</sup> Body Effects (Sun, Moon)
- Site Configurations:
  - Scenario 1:
    - Site 1 - Colorado Springs CO USA [39.01319824, -104.82175868, 2033.321m]
    - Site 2 - El Paso TX USA [31.762465, -106.247808, 1194.718m]
    - Site 3 - Arm MS USA [31.50000, -90.000000, 53.825m]
    - Average separation distance between sites = 1309.928km
  - Scenario 2:
    - Site 1 - Colorado Springs CO USA [39.01319824, -104.82175868, 2033.321m]
    - Site 2 - Pueblo CO USA [38.306790, -104.57815800, 1479.404m]
    - Site 3 - Yoder CO USA [38.700000, -104.18220700, 1661.043m]

- Average separation distance between sites = 67.485km
- Scenario 3:
  - Site 1 - Colorado Springs CO USA [39.01319824, -104.82175868, 2033.321m]
  - Site 2 - Colorado Springs CO USA [38.81783847, -104.85838552, 1861.446m]
  - Site 3 - Colorado Springs CO USA [38.84014924, -104.71511694, 1879.157m]
  - Average separation distance between sites = 18.648km

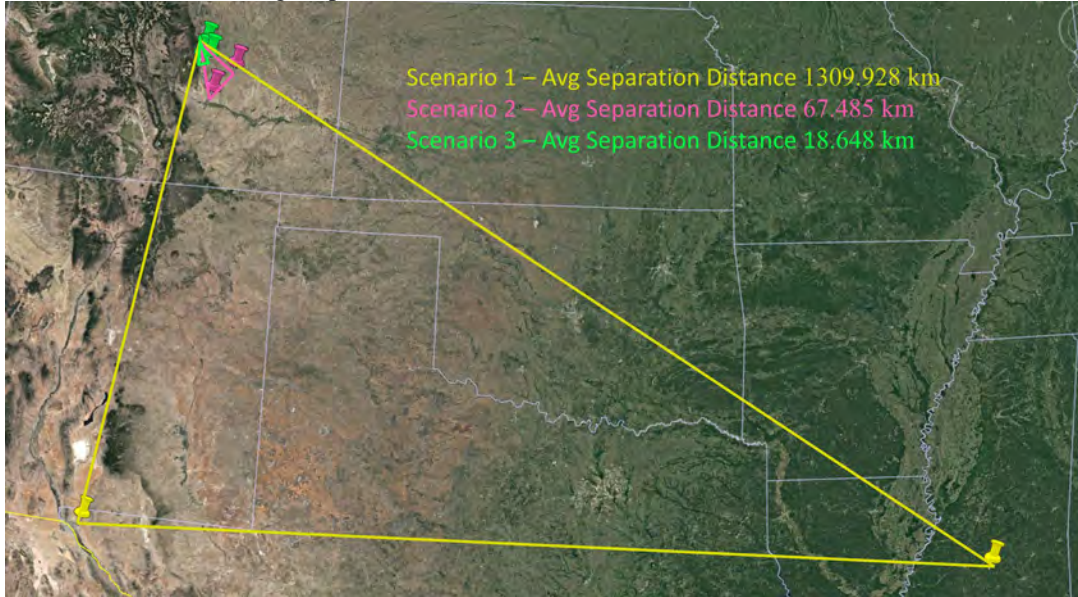


Fig. 4. Scenario Configurations

OREKIT was used as the simulation tool to provide the simulation of a LEO orbit by propagating 24 hours with a 5 second step size. Only when the satellite had an elevation above  $15^\circ$  were TDOA and FDOA measurements generated. TDOA and FDOA measurements were generated using a homegrown simulation capability in Python. The TDOA and FDOA measurement generator has been validated with real data at GEO. The measurements were then processed through an orbit determination system using a Gauss-Newton algorithm, which is an iterative approach to minimizing the residual sum of squares over the measurements. The generated state vector is then compared to the simulated data which is treated as truth to generate the error. Systems Tool Kit (STK) was used to plot the scenario site locations. A block diagram of the simulation architecture configuration can be seen in Fig. 5.

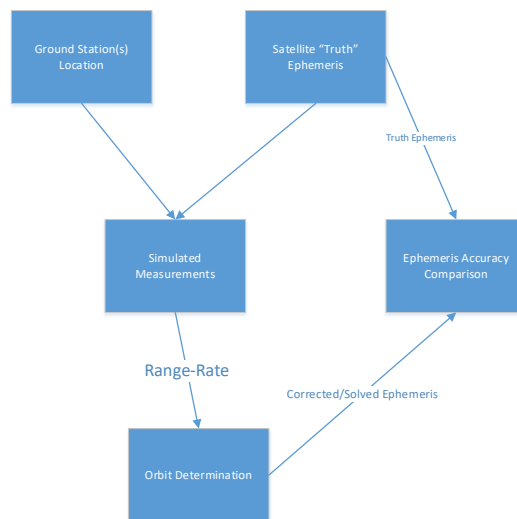


Fig. 5. Simulation Architecture

Scenario 1 was simulated to show how site geometry does not contribute significantly to the solution of a LEO satellite due to the motion of the satellite. This is important because the beam of a LEO satellite will not always be large depending on the altitude and the antenna on the satellite. So, the closer the sites can be, the easier to collect more passes. Fig. 6 shows a the STARLINK-1257 satellite with an antenna beam with of  $120^\circ$  with an altitude of approximately 570km. This image shows that the three ground stations are barely in the downlink beam with a large beam. This scenario may not be fully realistic due to the beam width but is being used to set a baseline of how the site geometry does or does not noticeably change the solution.

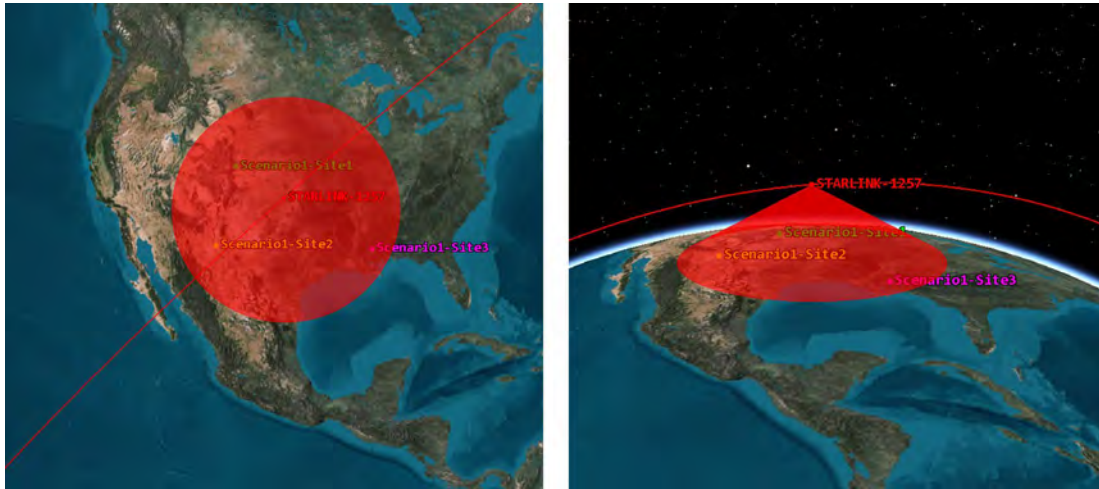


Fig. 6. Scenario 1 Configuration and Satellite Beam Projection

The average distance between the sites in Scenario 1 was 1309.928km. Due to this separation, only 142 measurements were able to be generated using the  $15^\circ$  elevation limit for each site. The resulting state vector from the orbit determination was compared with the truth data and generated an average error of 24.09km over a 24hr period of propagation. Fig. 7 shows the error of the generated solution compared to the truth data over the sample time.

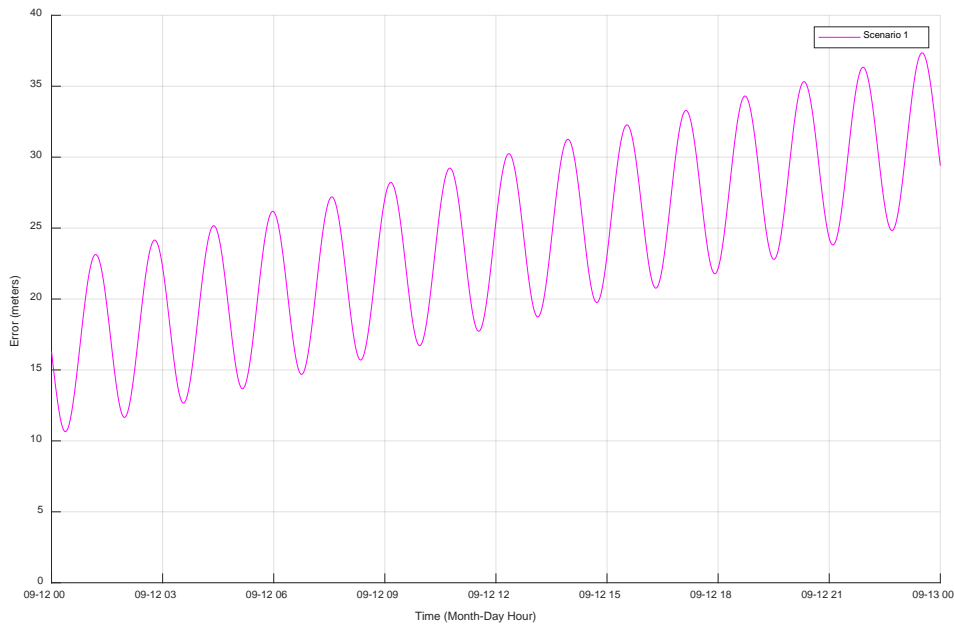


Fig. 7. Scenario 1 Error

Scenario 2 was simulated using a smaller geometry for the sensor sites, but the satellite was kept the same. The average distance between the sites in Scenario 2 was 67.485km. Due to this separation, 274 measurements were able to be generated using the 15° elevation limit for each site. The resulting state vector from the orbit determination was compared with the truth data and generated an average error of 19.56km over a 24hr period of propagation. Fig. 8 shows the error of the generated solution compared to the truth data over the sample time.

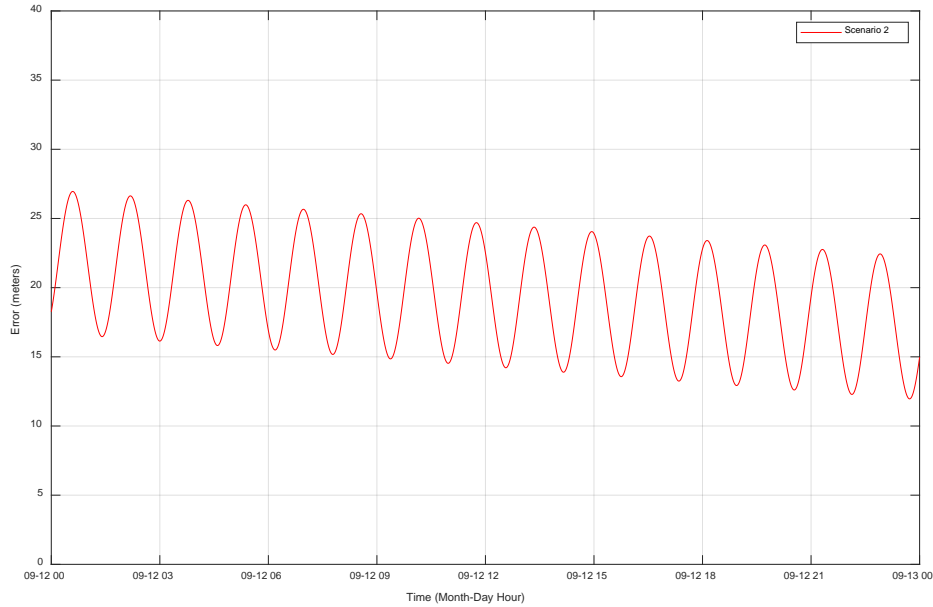


Fig. 8. Scenario 2 Error

Scenario 3 was simulated using the smallest geometry for the sensor sites, but the satellite was kept the same. The average distance between the sites in Scenario 3 was 18.648km. Due to this separation, 279 measurements were able to be generated using the 15° elevation limit for each site. The resulting state vector from the orbit determination was compared with the truth data and generated an average error of 19.56km over a 24hr period of propagation. Fig. 9 shows the error of the generated solution compared to the truth data over the sample time.

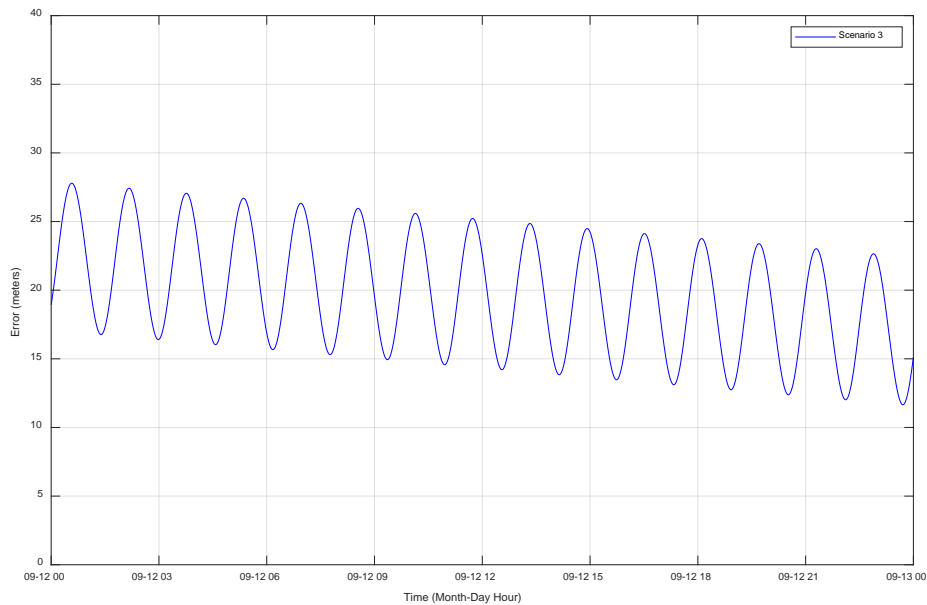


Fig. 9. Scenario 3 Error

Comparing the results of the scenarios shows that the results do not differ significantly based on the spacing of the sites. This allows sensors to be spaced closer together to track LEO satellites using traditional TDOA/FDOA methods. The next step of this simulation would be to add in Drag modeling to the truth data and the orbit determination method and then move on to real world collections. Fig. 10 shows the comparison of all the scenarios.

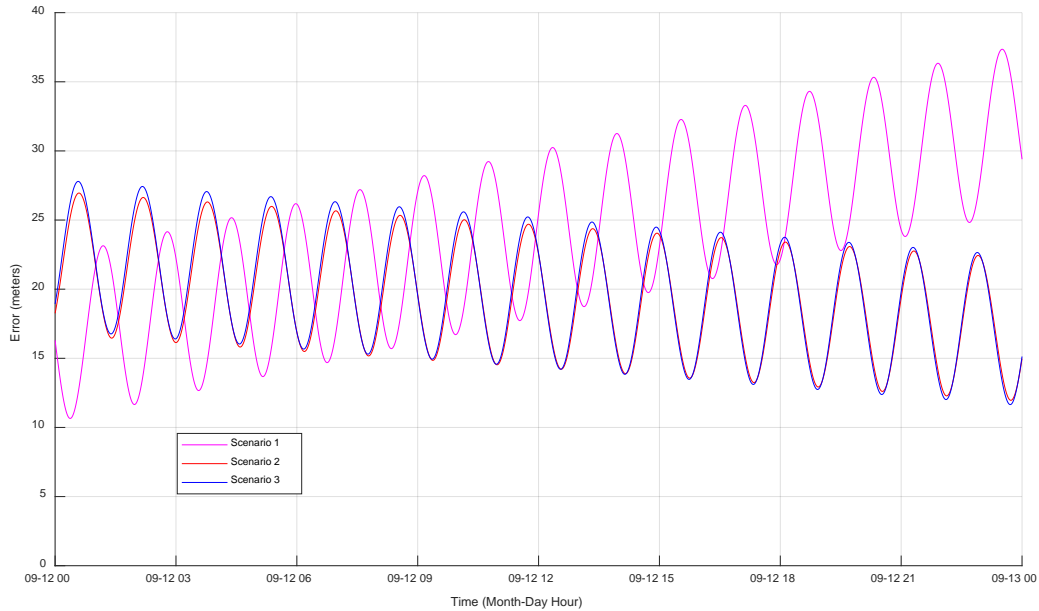


Fig. 10. All Scenario Errors

### *Doppler Shift Tracking*

This section will assess how Doppler Shift could be used to track satellites using a single aperture in LEO orbits. This has not yet been done in practice and is therefore simulation-based in this paper to determine if using the method in LEO is feasible. The data simulated here utilized an old orbit location for a Starlink satellite.

- Satellite:
  - Starlink-1257 (NORAD ID: 45402)
    - Epoch: 2020-09-12 18:00:15 UTC
    - X: -5500805.8784073368 (m)
    - Y: 3590624.2939960845 (m)
    - Z: 2193851.0305698211 (m)
    - Xdot: -1060.9082903965 (m/s)
    - Ydot: -5045.4521102592 (m/s)
    - Zdot: 5570.2825003079 (m/s)
- Orbit Perturbations:
  - (70x70) EGM-96 Earth Gravity Model
  - 3<sup>rd</sup> Body Effects (Sun, Moon)
- Ground Site:
  - Colorado Springs Colorado USA
- Downlink Access Times:
  - 1<sup>st</sup> Pass -> 2020 Sep 12 18:00:15.000 to 2020 Sep 12 18:12:05.000
  - 2<sup>nd</sup> Pass-> 2020 Sep 12 19:40:37.000 to 2020 Sep 12 19:51:37.000

OREKIT was used as the propagator in these simulations to provide a realistic high fidelity simulation result of the LEO satellite. The look angles for the satellite were also generated using OREKIT and plotted in Systems Tool Kit (STK) for visualization. This can be seen in Fig. 11, which shows the first pass over Colorado Springs.

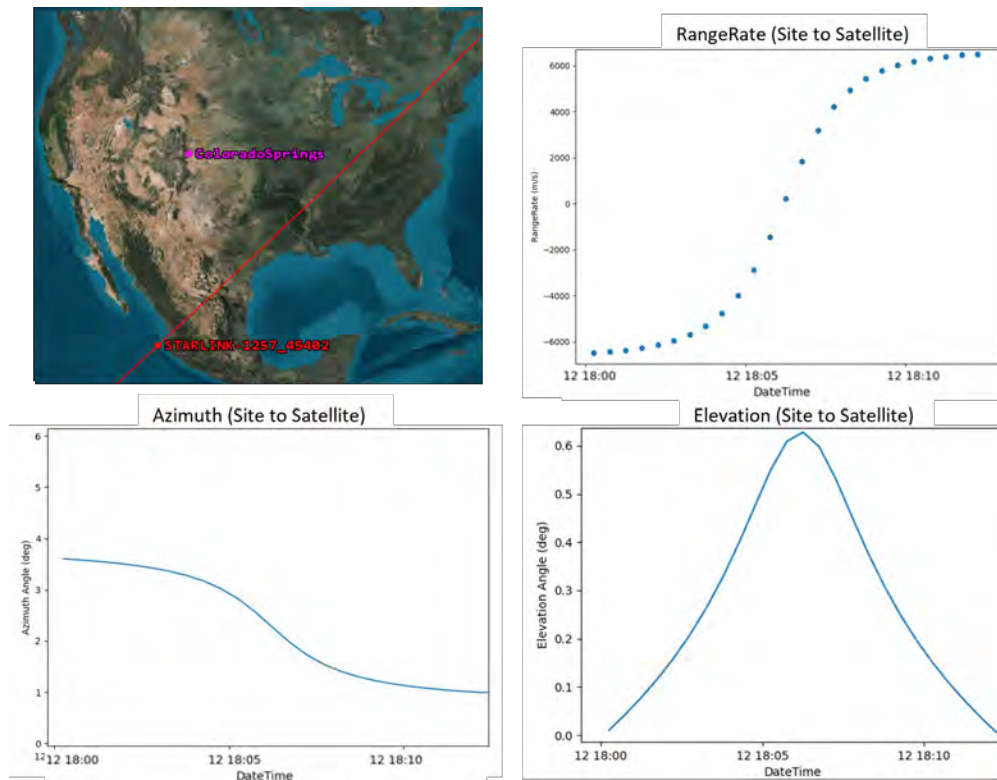


Fig. 11. Starlink-1257 1<sup>st</sup> Pass

Range rate is calculated using the satellite’s orbit, ground site location, and the assumed transmit and receive frequency. Once the data was simulated using OREKIT to propagate the satellite and compute look angles from the ground site, signals were modeled to compute the Doppler Shift. The Doppler shift was then transformed into Range-Rate simulated data using the following equation:

$$\text{RangeRate} = (f_{Tx} - f_{Rx}) \frac{c}{f_{Tx}}$$

$f_{Tx}$  – transmit frequency  
 $f_{Rx}$  – receive frequency  
 $c$  – speed of light

The Range-Rate is used in a special Range-Rate only orbit determination algorithm. The goal of this algorithm is to “correct” or create a better estimate than the initial given estimate of a single 6 element (X, Y, Z, Xdot, Ydot, Zdot) state vector by iteratively reducing and minimizing the sum of the squared error between observed measurements and theoretical measurements (residuals). A block diagram of the orbit determination process can be seen in Fig. 12

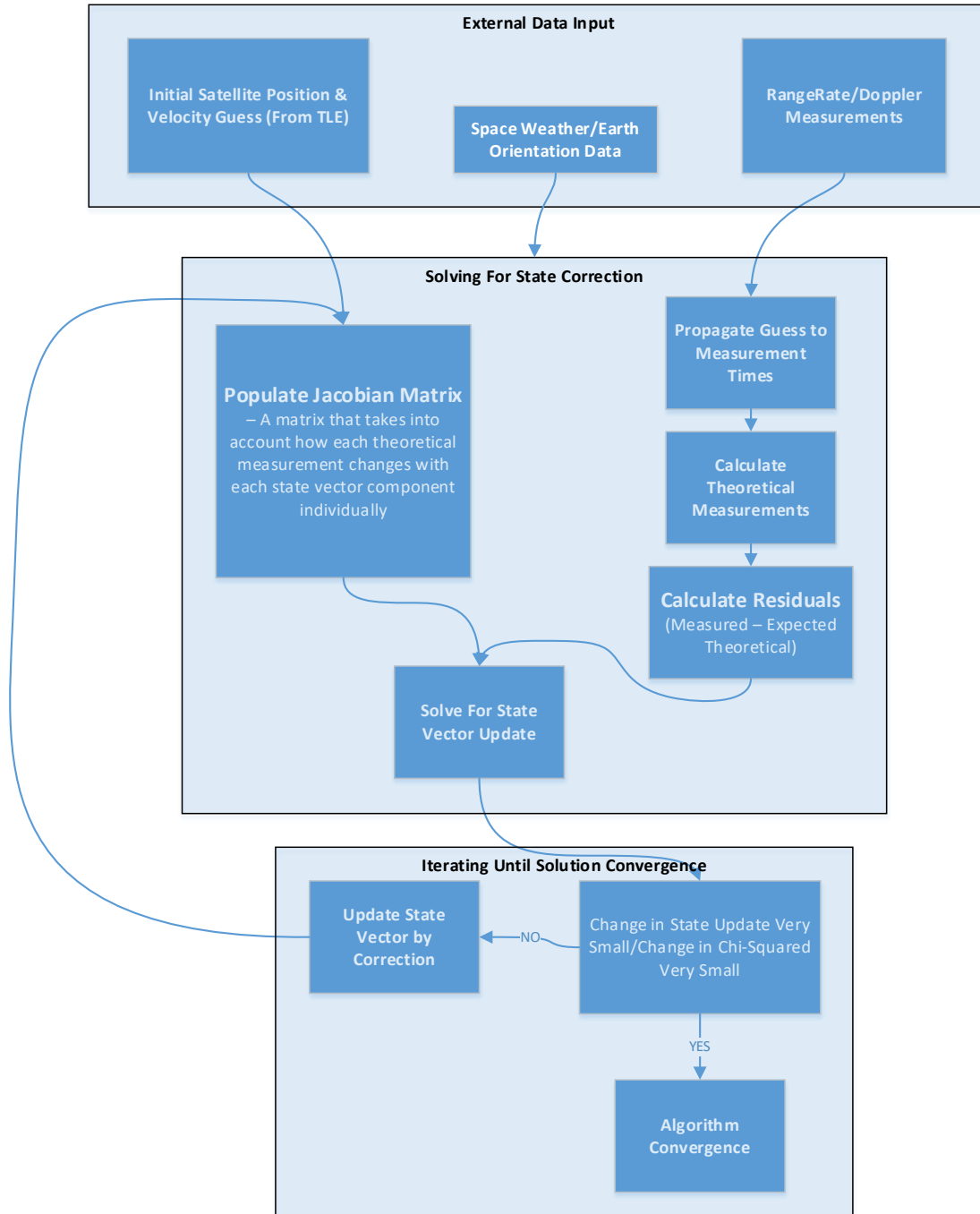


Fig. 12. Orbit Determination Process

Using 40 “perfect” simulated range rate measurements separated by 30 second time steps from two passes of the satellite, the orbit determination algorithm converges to a “perfect” solution (~0 meters error) even when starting with an initial guess for the satellite’s location that is ~341 km off in the in-track direction (45 seconds of error along the satellite’s orbit) from the true location. It is significant, because it proves Range Rate / Doppler measurements from a single aperture and single site can be used to correct ephemeris in ideal conditions. The next step is to take this from simulation to real world collection and compare against GPS ephemeris.

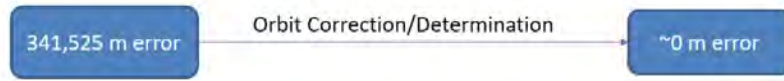


Fig. 13. Results

## 5. CONCLUSION

This paper describes how passive RF should be used to blind-scan satellites to identify, characterize, and track the signals being transmitted from the satellite. Passive RF can use SEI to uniquely identify satellites in a cluster of satellites and passive RF can also be used to blind scan satellites to find signals of interest from satellites. The paper also describes two different methods that could be used to process passive RF data to generate state vector data for LEO satellites. This demonstrates that passive RF ranging serves as a valuable technology in support of the SDA mission.

## 6. REFERENCES

- [1] J.M. McGinthy, L.J. Wong, A.J. Michaels. Groundwork for Neural Network-Based Specific Emitter Identification Authentication for IoT. *IEEE Internet of Things Journal*, Vol. 6, No. 4, August 2019.
- [2] Y. Lin, J. Jia, S. Wang, B. Ge, S. Mao. Wireless Device Identification Based on Radio Frequency Fingerprint Features. *IEEE Xplore*.